

Computations for a Breast Ultrasonic Imaging Technique and Finite Element Approach for a Fractional Derivative Modeling the Breast Tissue Acoustic Attenuation

Aïcha Bounaïm¹ and Wen Chen²

¹Schlumberger Stavanger Research
Risabergveien 3, Tananger
P.O. Box 8013, 4068 Stavanger, Norway
bounaima@yahoo.com

²Department of Engineering Mechanics
Hohai University, Xikang Road No.1 Nanjing,
Jiangsu Province 210098, China
chenwen@hhu.edu.cn

ABSTRACT

Biomathematics use mathematics to quantitatively represent the dynamics of biological or biomedical systems and thereby analyze and predict system behavior. This work addresses an application of bioacoustic modeling and computations to a clinical imaging technique for breast cancer detection. The mathematical model consists in a damped wave equation incorporating a frequency-dependent attenuation, which describes ultrasound propagating in the human breast tissue. 3D numerical simulations are presented to investigate the detectability of breast tumors. An extension to a more general model for the acoustic attenuation is also discussed. For this, 2D numerical experiments are presented to illustrate the issue in the case of the CARI technique.

Keywords: breast cancer detection, ultrasound propagation, fractional derivative for acoustic attenuation.

2000 Mathematics Subject Classification: 92B05.

1 Introduction - Clinical description

Breast cancer became the most widespread female disease, in particular in western countries. Lives can be saved and treatment can be more effective if the diagnosis is made early. Ultrasonography is a common technique used in breast screening due to its low cost and large availability. Moreover, it is a good adjunct to mammography in differentiating cancerous from non-cancerous breast tumors. In this study, we are interested in the CARI (clinical amplitude-velocity reconstruction imaging) ultrasonic technique that was developed by Dr. K. Richter [8, 9].

The breast, in the CARI device, is fixed between two plates as schematically illustrated in Figure 1. The stainless steel plate, opposite to the transducer, plays the role of a reference structure

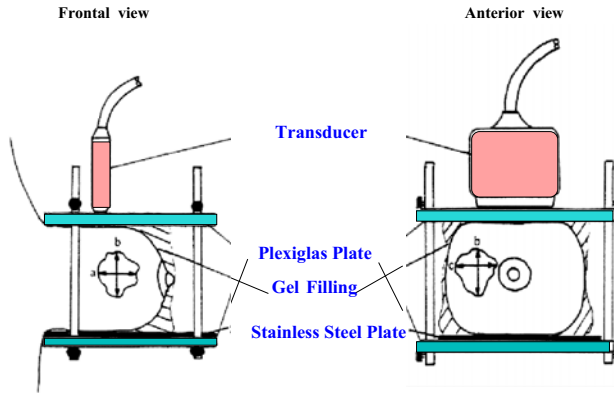


Figure 1: Two frontal views of the ultrasonic CARI technique for breast tumor detection taken from [9].

producing a reflecting line (RL). The CARI modality operates in such that the RL is straight if the sound velocity in the intervening tissues is roughly homogeneous while it is elevated if the tissue contains a suspicious tumor as shown from the CARI-ultrasonic image in Figure 2. The CARI technique is characterized by two important acoustic components of breast evaluation, namely the sound speed and the attenuation. Moreover, the CARI method is more sensitive than the conventional ultrasound, especially in assessing cancer surrounded by the breast fatty tissue.

In general, experimental study in living tissues is not practical, and acoustic phantoms are useful but limited. Therefore, mathematical computer modeling of ultrasound propagation and scattering complement to both approaches, although it has its own limitations. Moreover, recent advances in high-performance computing enable large-scale simulations such those occurring in high frequency acoustic wave propagation.

2 Mathematical and geometrical modeling

To simulate ultrasound in breast models taking into account the two tissue parameters of the CARI technique, we solve the damped linear wave equation in an inhomogeneous lossy acoustic medium representing the breast fatty tissue:

$$\frac{1}{c^2} \frac{\partial^2 p}{\partial t^2} + \gamma \frac{\partial p}{\partial t} = \nabla^2 p, \quad (2.1)$$

where p is the pressure, c is the sound velocity, and γ is the damping or attenuation parameter. Note that wave attenuation is an essential tissue characteristic. There are various attenuation mechanisms where few of them can be isolated, and commonly the attenuation follows a power law in frequency f expressed as

$$\gamma = \alpha f^y, \quad (2.2)$$

where coefficients α and y depend on the tissue. For example, in water $\alpha \approx 0.0022\text{dB/cm/MHz}^y$, $y = 2.0$, and in muscle tissue $\alpha \approx 0.7\text{dB/cm/MHz}^y$, $y = 1.1$. In our simulations, $\alpha = 2\alpha_0/c$ and

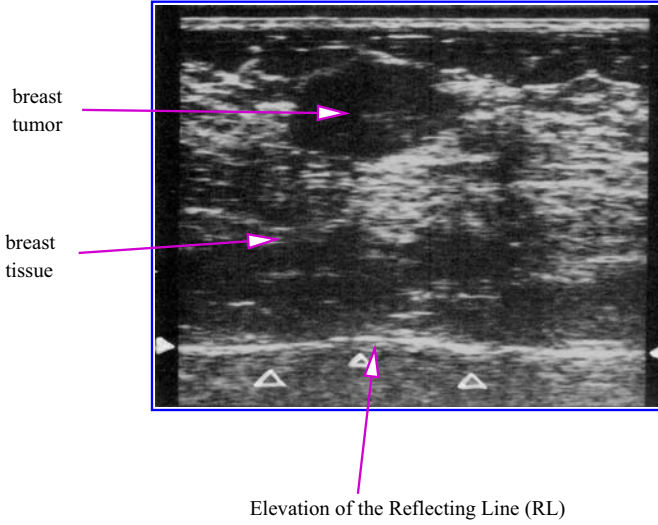


Figure 2: A CARI-ultrasound image showing the elevation of the reflecting line due to the presence of a tumor in the breast tissue.

the values of c , α_0 and γ are deduced from clinical experiments and will be specified later. In the last section we introduce a more general attenuation model using Laplacian fractional derivative.

The equation (2.1) is supplemented with initial and boundary conditions according to the 3D configuration in Figure 3. The transducer is represented by a Dirichlet condition

$$p(x_{\text{trsd}}, t) = p_{\text{trsd}}(x, t). \tag{2.3}$$

The RL in the CARI setup is modeled by reflecting boundary (RB) conditions

$$\frac{\partial p}{\partial n}(x_{\text{RB}}, t) = 0, \tag{2.4}$$

while the remaining boundaries are represented by first-order absorbing or non-reflecting boundary (NRB) conditions:

$$\frac{\partial p}{\partial n}(x_{\text{NRB}}, t) = -\frac{1}{c} \frac{\partial p}{\partial t}. \tag{2.5}$$

The system is initialized with the conditions:

$$p(x, t_0) = p_{\text{atm}} \quad \text{and} \quad \frac{\partial p}{\partial t}(x, t_0) = 0. \tag{2.6}$$

The FETD (finite element time domain) approach used to discretize the equation (2.1) and the corresponding boundary conditions consists of a finite element method in the spatial domain and a second order finite difference representation to evaluate the time derivatives. A semi-discrete time scheme of (2.1) writes

$$\frac{p^{n+1} - 2p^n + p^{n-1}}{\Delta t^2} + \gamma c^2 \frac{p^{n+1} - p^{n-1}}{2\Delta t} = c^2 \nabla^2 p^n, \tag{2.7}$$

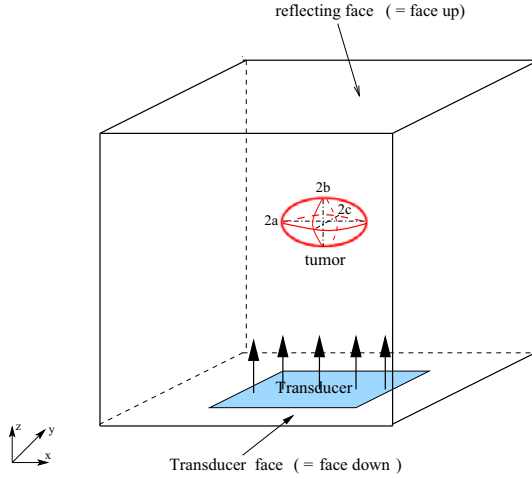


Figure 3: 3D configuration of the CARI technique for ultrasound breast tumor detection

where Δt is the time step size and the superscript n denotes the n th time iterate of the pressure field. Then, by decomposing p^n in a finite element basis and incorporating the boundary conditions, (2.7) leads to

$$A_1 p^{n+1} = A_2 p^n + A_3 p^{n-1}, \quad (2.8)$$

where the matrices A_i , ($i = 1, 2, 3$) result from the finite element matrices and depend on the parameters c , γ , and Δt . In summary, the problem is reduced to the solution of a linear system at each time step. The numerical implementation is carried out using *Diffpack*, a finite element library based on C++ and object-oriented programming [7]. We refer to [3] for a detailed description of the FETD discretization method as well as a review on the stability of the numerical scheme.

3 Numerical results and discussions

Geometrically, the breast tissue is assimilated to a 3D box of size 22mmx24mmx20mm containing an ellipsoid-shaped tumor of axes 2a, 2b and 2c as shown in Figure 3. The transducer is a 12mmx8mm-rectangle from which a 3.5MHz signal is transmitted into the breast tissue. The sound speed in the breast tissue and the tumor are extracted from clinical experiments [10] together with the attenuation parameters, and are summarized in Table 1. Note that the transducer signal has a wavelength of $\lambda = \frac{f}{c} \approx 0.4\text{mm}$. Thus, for a better resolution of the spatial features, a grid is chosen able to resolve 2 finite elements per wavelength which requires a grid of approximately 1.5×10^6 nodes. The numerical scheme is then stable for a time step $\Delta t = 26 \times 10^{-9}\text{s}$, and two ways of the wave traveling along the 3D breast model is achieved over 1125 time steps.

As shown in Figure 5, the waves are perturbed due to the presence of the tumor in the abnormal tissue compared to the healthy (or homogeneous) one. Here, the tumor is an ellipsoid of axes

Table 1: Sound velocity and coefficients of frequency-dependent power law attenuation of the breast tissue and tumor.

	breast fatty tissue	breast cancer
$c(\text{m/s})$	1475	1527
$\alpha_0(\text{dB/MHz}^\gamma)$	15.8	57.0
$\gamma(\text{s/m}^2)$	1.7	1.3

(12mm,8mm,8mm), and the views represent cross-sections normal to the wave propagation direction.

Clinically, the ultrasound imaging techniques have some limitations and lesions as small as 1cm-diameter can hardly be detected. The numerical experiments show instead that smaller lesions can be readily recognized in the tissue, an observation confirmed by 2D simulations in [3], which mimic cross-sections in 3D breast model.

Besides the disturbance of the echo pattern around the lesion, snapshots from Figure 5 show that the ultrasound pressure is attenuated as the wave propagates along the tissue towards the RL and back to the transducer. Moreover, ultrasound pressure of a layer traversing the tumor ($z=5\text{mm}$) displayed at successive time steps on Figure 7 gives a quantitative evaluation in detecting the tumor and recognizing its shape.

4 On a fractional derivative attenuation model

Acoustic waves propagating in media exhibiting arbitrary frequency power law attenuation can be modeled by time-domain partial differential equations given by (2.1). However, for non-integer power exponent γ of the attenuation parameter γ , these models may not accurately describe more realistic media such as soft biological tissues. Therefore, we introduce in this section a new model for the dissipative term using a Laplacian fractional derivative developed by Chen and Holm [5, 6]:

$$\frac{1}{c^2} \frac{\partial^2 p}{\partial t^2} + 2 \frac{\alpha_0}{c^{1-\gamma}} \frac{\partial}{\partial t} ((-\Delta)^{\gamma/2}) = \nabla^2 p, \tag{4.1}$$

where the coefficients are similar to those introduced earlier. Chen and Holm note that the spatial fractional Laplacian models reflect the fractal microstructures of the media and describe quite well the frequency power law attenuation.

We aim in this section to develop a finite element approach to the new wave equation.

Using a finite element approach to the equation (4.1) and the Green's formula for the right hand side term, we assume we obtain the *pseudo-spatial approximation*:

$$\frac{1}{c^2} \frac{\partial^2 (Mp)}{\partial t^2} + 2 \frac{\alpha_0}{c^{1-\gamma}} \frac{\partial}{\partial t} (K^{\gamma/2} p) = -Kp + Bp. \tag{4.2}$$

The matrices M , K , and B are given, respectively, by

$$[M_{ij}] = \int_{\Omega} N_i N_j dx, \quad [K_{ij}] = \int_{\Omega} \nabla N_i \nabla N_j dx, \quad [B_{ij}] = \int_{\partial\Omega_{NR}} N_i N_j d\sigma, \tag{4.3}$$

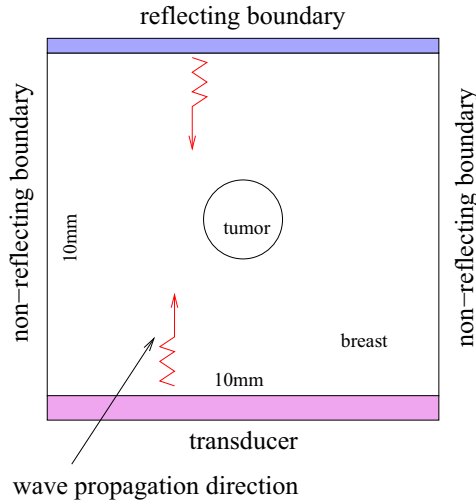


Figure 4: 2D configuration used for the FEM simulations of the wave propagating in attenuated medium

where N_i are the finite element basis functions and ∇N_i their gradients. Ω_{NR} refers to as the non-reflecting boundaries of the computational domain as illustrated on Figure 4.

Then, using a second-order finite difference approximation in time, we get the discrete matrix form

$$\begin{aligned} \left[2M + 2\alpha_0 c^{1+y} \Delta t K^{y/2} + c \Delta t B \right] p^{n+1} = & -2c^2 \Delta t^2 K p^n + 4M p^n - 2M p^{n-1} \\ & + 2\alpha_0 c^{1+y} \Delta t K^{y/2} p^{n-1} + c \Delta t B p^{n-1}. \end{aligned}$$

The pressure is then calculated by a process solving a linear system at each time step.

4.1 Some 2D numerical results

To our knowledge, numerical simulations involving fractional derivative are not widely treated in the literature. In this section, we investigate the feasibility of the finite element approach to give quantitative results on the behavior of the wave propagating in media presenting a fractional derivative attenuation model. We especially study the effect of the power exponent y on the presence or not of the oscillations within or outside the tumor region.

The domain is a 10mmx10mm square meshed with a 26x26nodes-grid, the sound speeds in the breast and the tumor respectively are $c_{\text{breast}} = 1475 \text{ms}^{-1}$, $c_{\text{tumor}} = 1527 \text{ms}^{-1}$, and $\alpha_0 = 1$ is the first attenuation coefficient. The matrix $K^{y/2}$ is computed using one of the matrix functionalities of MatLab. The process is time consuming and results, in particular, in a full matrix.

Two series of numerical experiments are carried out for different values of y when the wave travels in the 2D breast model outside the tumor region: (1) for 5 values of y close to 0, Figure 8 shows that the oscillations are very similar; (2) for 5 values of y between 0.2 and 2, the results from Figure 9 show that the oscillations are present for $y=0.2$ and $y=0.5$, but then

disappear when $\gamma \geq 1$. It is also observed that the amplitude is smaller than the above case. In Figures 10 and 11, the same observations are made from the results when the wave propagates across the tumor region. Other results are presented in [4].

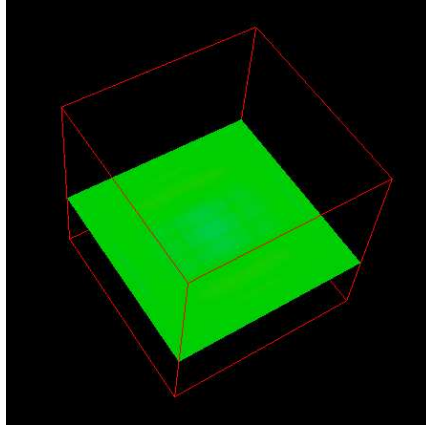
5 Conclusions and perspectives

This paper addresses bioacoustic numerical modeling for the CARI ultrasonic breast imaging technique. A finite element approach is presented and numerical experiments for a 3D breast model illustrate the detectability of lesions in the breast fatty tissue.

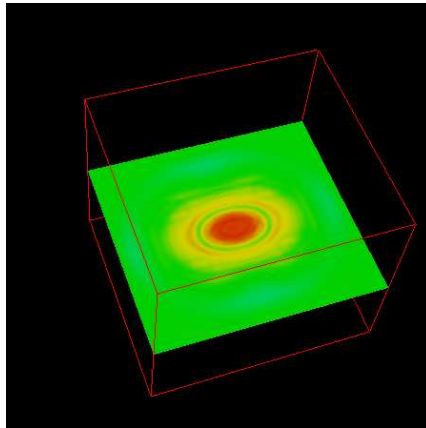
The attenuation model is extended by introducing a Laplacian fractional derivative. The discretization of the wave equation incorporating the new attenuation model is achieved by a finite element method. The numerical results, although limited to bi-dimensional case and simple boundary conditions, give insights in the feasibility of the attenuation modeling in human soft tissues. However, further analysis can be done to achieve a more accurate numerical approximation of the presented attenuation model.

References

- [1] A. Bounaïm, S. Holm, W. Chen, Å. Ødegård, A. Tveito and K. Thomenius, FETD simulation of wave propagation modeling the CARI breast sonography, Proc. ICCSA'2003, LNCS 2668, pp. 705-714, Springer-Verlag, 2003.
- [2] A. Bounaïm, S. Holm, W. Chen, and Å. Ødegård, Sensitivity of the ultrasonic CARI technique for breast tumor detection using a FETD scheme, Journal Ultrasonics, Vol 42, Issues 1-9, pp. 919-925, 2004.
- [3] A. Bounaïm, S. Holm, W. Chen, and Å. Ødegård, Quantification of the CARI breast imaging sensitivity by 2D/3D numerical time-domain ultrasound wave propagation, J. Mathematics and Computers in Simulation, Vol 65, Issues 4-5, pp. 521-534, 2004.
- [4] A. Bounaïm, S. Holm, W. Chen and Å. Ødegård, Modified fractional derivative model for the attenuation of acoustic waves propagating in human soft tissue: Finite element simulations using Diffpack, Simula Report 2004-02, Simula Research Laboratory, 2004.
- [5] W. Chen and S. Holm, Modified Szabo's wave equation models for lossy media obeying frequency power law, J. Acoust. Soc. Amer., 114(5), pp. 2570-2584, 2003.
- [6] W. Chen and S. Holm, Fractional Laplacian time-space models for linear and nonlinear lossy media exhibiting arbitrary frequency dependency, J. Acoust. Soc. Amer., 114(5), pp. 1424-1430, 2004.
- [7] H.P. Langtangen, Computational partial differential equations - Numerical methods and Diffpack programming, Springer-Verlag, 1999.
- [8] K. Richter and SH. Heywang-Köbrunner, Quantitative parameters measured by a new sonographic method for detecting breast lesions, Invest. Radiol., Vol 30, pp. 401-411, 1995.

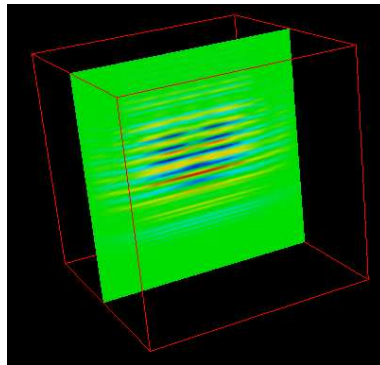


(a)

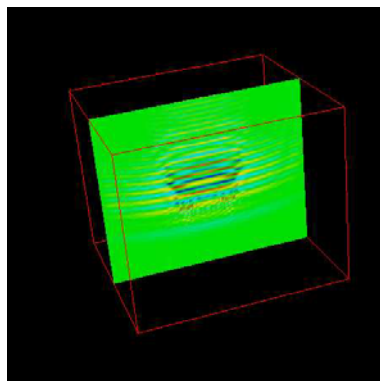


(b)

Figure 5: Ultrasound pressure in a cross-section ($z=7\text{mm}$) normal to the z -axis and traversing the tumor for two breast fatty tissues at $t=23.9\mu\text{s}$: (a) homogeneous tissue; (b) containing a $(12\text{mm},8\text{mm},8\text{mm})$ -ellipsoid tumor. The shape of the section is readily recognized in the background medium.



(a)



(b)

Figure 6: Ultrasound pressure in a cross-section normal to the y -axis and traversing the tumor for two breast fatty tissues at $t=23.9\mu s$: (a) homogeneous tissue; (b) containing a (12mm,8mm,8mm)-ellipsoid tumor. The wave travels back to the transducer, and it is noted that it is disturbed around the tumor compared to the tissue without tumor.

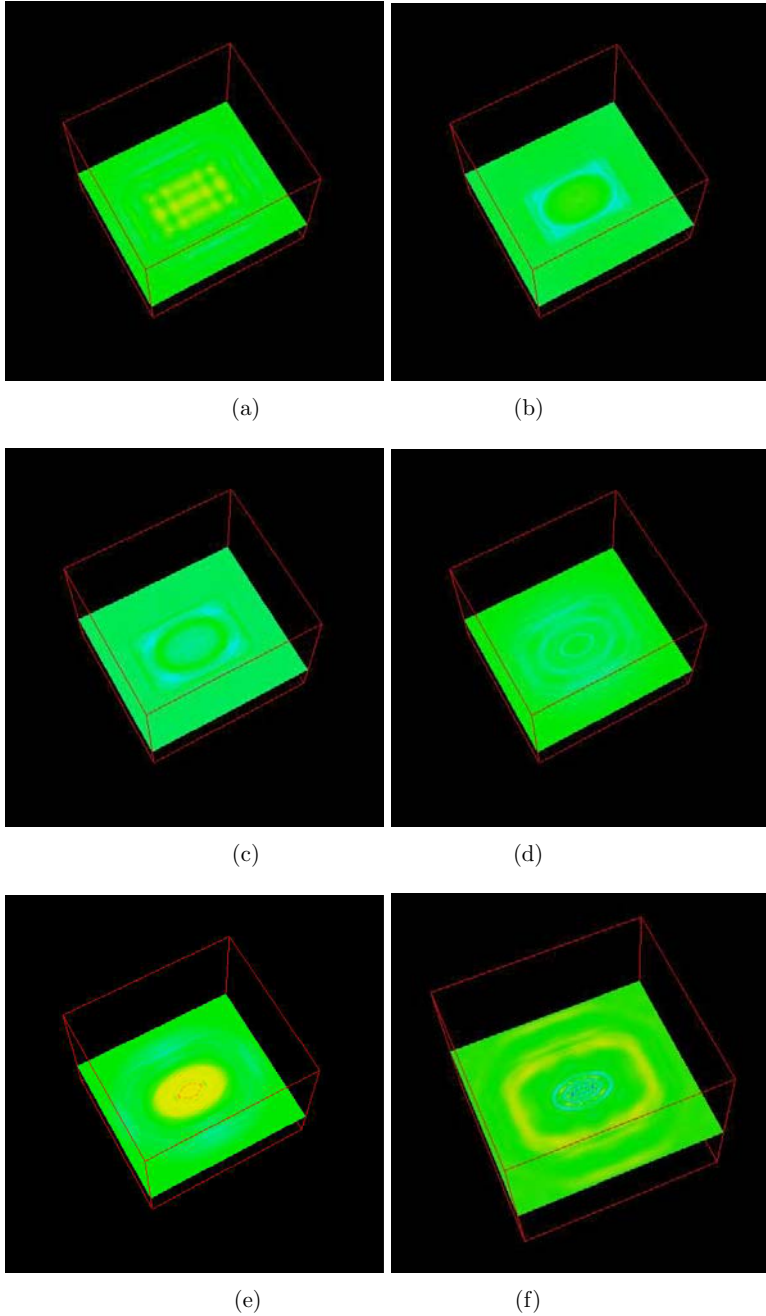


Figure 7: History of the ultrasound pressure in the breast tissue containing an ellipsoid tumor at 8 successive time steps:(a) $t=26.6\text{ns}$; (b) $t=2.6\mu\text{s}$; (c) $t=7.9\mu\text{s}$; (d) $t=15.9\mu\text{s}$; (e) $t=18.6\mu\text{s}$; (f) $t=29.3\mu\text{s}$. The color scale shows also the attenuation of the pressure during the two-way travel of the wave along the tissue.

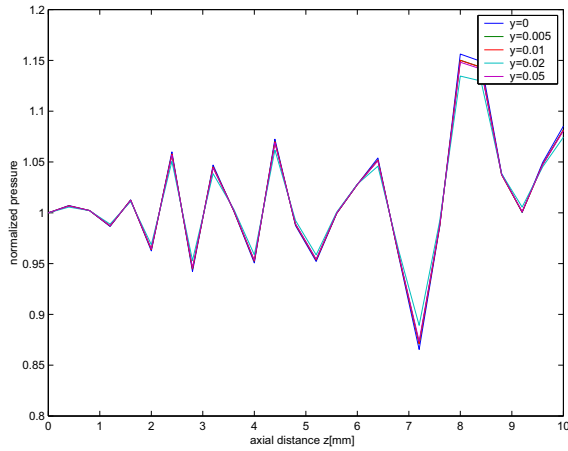


Figure 8: Normalized ultrasound pressure in 5 different media presenting a fractional Laplacian derivative attenuation model. The media are varying according to 5 values (close to 0) of the power exponent parameter y . The plots represent the pressure field as a function of the axial distance (z) when the lateral distance is fixed to $x=-3\text{mm}$, i.e., the wave travels outside the tumor region.

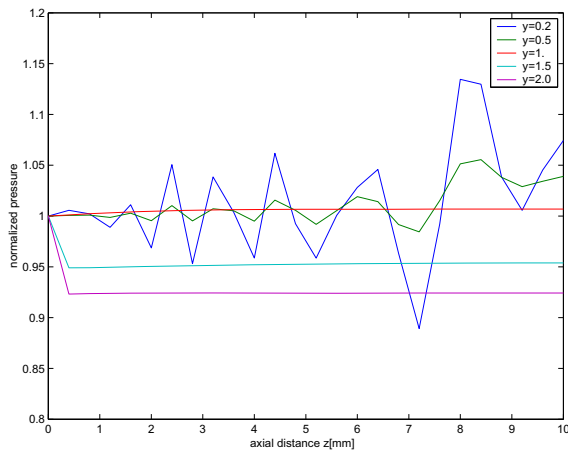


Figure 9: Normalized ultrasound pressure in 5 different media presenting a fractional Laplacian derivative attenuation model. The media are varying according to 5 values (between 0.2 and 2) of the power exponent parameter y . The plots represent the pressure field as a function of the axial distance (z) when the lateral distance is fixed to $x=-3\text{mm}$, i.e., the wave travels outside the tumor region.

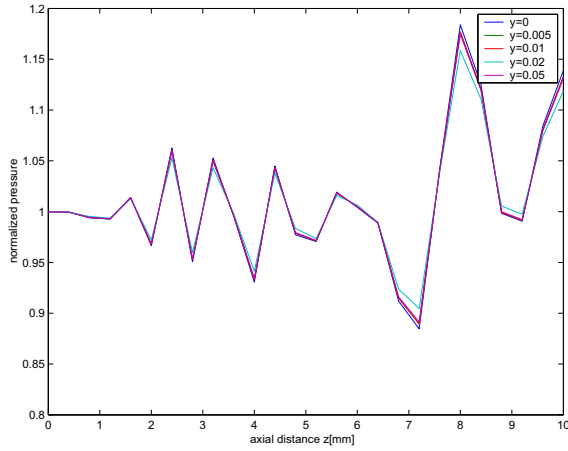


Figure 10: Normalized ultrasound pressure in 5 different media presenting a fractional Laplacian derivative attenuation model. The media are varying according to 5 values (close to 0) of the power exponent parameter y . The plots represent the pressure field as a function of the axial distance (z) when the lateral distance is fixed to $x=1\text{mm}$, i.e., the wave travels through the tumor region.

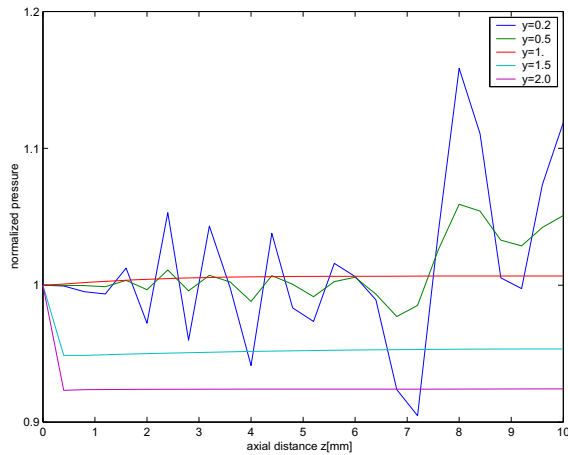


Figure 11: Normalized ultrasound pressure in 5 different media presenting a fractional Laplacian derivative attenuation model. The media are varying according to 5 values (between 0.2 and 2) of the power exponent parameter y . The plots represent the pressure field as a function of the axial distance (z) when the lateral distance is fixed to $x=1\text{mm}$, i.e., the wave travels through the tumor region.

- [9] K. Richter, Clinical amplitude/velocity reconstructive imaging (CARI)-a new sonographic method for detecting breast lesions, *The British Journal of Radiology*, Vol 68, pp. 375-384, 1995.
- [10] W. Weiwad, A. Heinig, L. Goetz, H. Hartmann, D. Lampe, J. Buchmann, R. Millner, R.P. Spielmann and S.H. Heywang-Koebrunner, Direct measurement of sound velocity in various specimens of breast tissue, *Investigative Radiology*, 35(12), pp. 721-726, 2000.